Stony Brook University

DEVELOPMENT OF IODINATED GRAPHENE NANOPLATELETS THROUGH REDOX REACTION FOR THEIR USE AS CT CONTRAST AGENTS

A Thesis Presented

by

Aditi Parag Gadgil

To

The Graduate School
in Partial Fulfillment of the
Requirements
for the Degree of

Master of Science

in

Biomedical Engineering

Stony Brook University

August 2013

Stony Brook University

The Graduate School

Aditi Parag Gadgil

We, the thesis committee for the above candidate for the

Master of Science degree, hereby recommend

acceptance of this thesis.

Dr. Balaji Sitharaman – Thesis Advisor

Assistant Professor, Biomedical Engineering

Dr. Terry Button - Chair of Thesis Committee

Associate Professor of Radiology, Stony Brook Medical Center

This thesis is accepted by the Graduate School

Charles Taber

Interim Dean of the Graduate School

Abstract of the Thesis

Development of Iodinated Graphene Nanoplatelets through Redox Reaction for their Use as CT Contrast Agents

by

Aditi Parag Gadgil

Master of Science

in

Biomedical Engineering

Stony Brook University

2013

Iodinated organic compounds currently dominate the market of contrast media for CAT imaging. When these compounds have to be used in large quantities for multiple CAT scans, it can result in adverse effects ranging from mild to severe. Secondly, iodine being the only element which gives the essential optical properties to the agent, large quantity of iodine is needed in preparing these compounds. Recently, graphene-based compounds are being researched for their exceptional optical properties, and their compatibility with the body tissues. If combined with iodine, they are believed to give a significant contrast with a less dose of the agent. In this thesis work, we tried to synthesize graphene nanoplatelets incorporating iodine ions through chemical bonding. We modified Hofmann's method[1] to oxidize graphite flakes; with a further modification of using potassium iodate in the place of potassium chlorate as an oxidizer, in order to attach iodine ions to the graphene oxide platelets. Later, we reduced these oxidized graphene platelets using 32.1 mM hydroiodic acid instead of the standard hydrazine. Dextran-coating was done to make the molecules more dispersible in water and also biocompatible with the body tissues. The efficiency of the chemical reactions was examined by different characterization techniques like Raman Spectroscopy, UV-Vis spectroscopy and ISE. The morphology was checked by TEM and AFM. The particle size obtained was in the range of 1 – 2 μm. Cell toxicity studies were done by the LDH and Prestoblue assay to evaluate the toxicity of the particles on two different cell lines. CT Phantom studies showed that the contrast produced by the composite material was more than an equivalent amount of pure iodine.

Contents

List of Figures

List of Tables

List of Abbreviations

1. CAT - Computed Axial Tomography
2. CA – Contrast Agent
3. ISE - Ion selective Electrode
4. TEM - Transmission Electron Microscopy
5. AFM - Atomic Force Microscopy
6. UV-Vis Spectroscopy - Ultra-violent Visible Spectroscopy
7. LDH - Lactate Dehydrogenase
8. GNP's - Graphene Nanoplatelets
9. HI- Hydroiodide
10. DI water - Deionised
11. Dex – Dextran
12. Dex-HI red GNPs – Dextran coated HI reduced Graphene Nanoplatelets
13. EMEM - Eagle's Minimum Essential Medium
14. DMEM - Dulbecco's Minimum Essential Medium
15. KMNO4 – Potassium Permanganate
16. KIO3 – Potassium Iodate

Acknowledgements

It was with a simple idea in mind “I need to have a thesis published in my name” that I started with this long-lasting task. Little did I know then, that it would require involvement of so many people and that it would not be correct on my part to call it only my thesis. I would like to express my gratitude to all those people, who have contributed in my thesis work directly and indirectly.

First and foremost, I want to profusely thank my research advisor, Dr. Balaji Sitharaman, for giving me such an interesting project to work upon. He has been an excellent mentor as he guided me through various fronts during my research, and provided me with his inputs now and again. He has been patient with all my mistakes, delays, and ignorance.

I am deeply thankful to Dr. Terry Button, who took out time from his busy schedule, for assisting me complete my thesis work, and agreeing to be on my thesis defense committee. He also helped to obtain valuable results for the final part of my project, which was carried out in the Medical Center of Stony Brook University. Louis and George, at the CAT Scanning Center, also helped me in obtaining important information about the results, and I would sincerely like to thank them too.

I would also like to thank Joe Livingston who had the preliminary data for the same project. His thesis gave me the starting point of the research for my thesis.

I am grateful to the people of Galbraith Laboratory, who in a timely manner submitted critical results for this project. I appreciate the efforts put in by all of them in such a short time.

My lab mates Gaurav Lalwani for giving me the TEM results and Sunny Patel for the SEM images; they have been a great help otherwise too. Inspite of pestering them with numerous questions, Shruti Kanakia and Sayan Mullick Chowdhary have helped me by answering all of them. Their knowledge and experience in research helped me tremendously in taking decisions about my research designs. Besides them, Yahfi Tahlukhdar, Behzaad Farshid, Stephen Lee, Jason Rashkow, Cassandra Suhrland, Shilpi Goenka, Justin Fang and all other students also contributed knowingly or unknowingly with their timely help. Also, the fun-filled environment that was created in lab, gave me the extra enthusiasm to work.

I also want to thank Sherlyn Divya from Material Science Department, who helped me use the UV-Vis spectrometer in her lab, with the permission of her advisor, Dr. Perena Gouma.

My friends, Rajvi Doshi, Saurabh Gandhi, Bharat Kapoor, Kelechi Nwachukwu and also my housemates showed lot of interest throughout my thesis work. They always kept a check on me for updates on my work and questioned me on certain points. That helped me to further

evaluate my own work, and try to solve issues, if any. Besides, they motivated me constantly to work hard.

I will always be grateful to my family in India which includes my mother, father, sister and my cousins. They have always been supportive and shown confidence in me to succeed in whatever path I choose.

1. INTRODUCTION

1.1 Computed Tomography

The diagnosis of soft tissue and vasculature can be done by various imaging techniques, Computed (Axial) Tomography or CT scanning being one of the easier and cheaper ones. In this technique, X-rays are passed through the desired part of the patient. Depending on the characteristics of tissue in that part, some amount of X-rays is absorbed by the tissue in the patient, and the remaining X-rays are transmitted through the body. These transmitted rays then fall upon a detector, and a projected 2-Dimensional image is formed on the film. The images are cross-sections, or thin slices of the person's body that is being scanned. The individual cross-sections are later computed to give a single compiled snap-shot of the imaged body part. These CT images help us to identify defects or abnormalities in the body if present. In comparison to the conventional X-ray imaging, CT gives sharper and more detailed images of the organs.

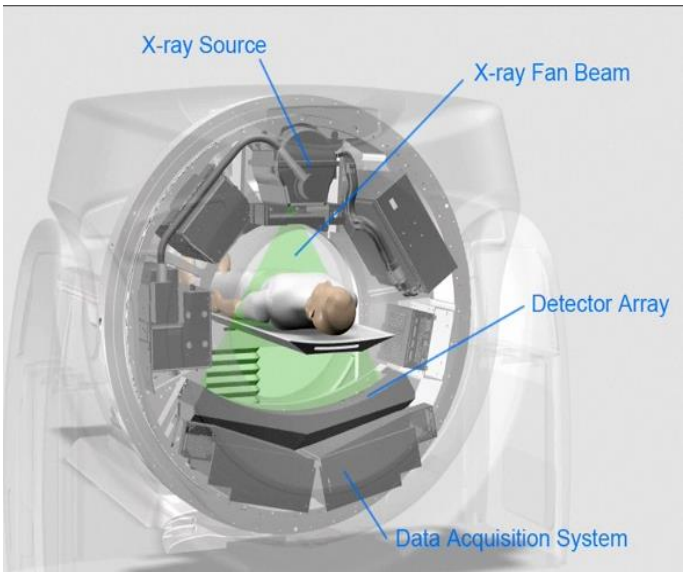

Figure 1: Computed Tomography Scanning Technique

Fig. 1 depicts the process of obtaining a CT scan[2]. The patient is placed in the center of the equipment. A beam of X-ray which can be as thick as 1 mm up to 10 mm is irradiated on the part of the patient's body which has to be imaged. The detector which is placed on the opposite side of the X-ray source captures all the radiations transmitted through the body, and different snapshots are recorded in several rotations of the X-ray tube. These snapshots are sent to the data acquisition system and compiled into one CT image.

1.2 Contrast Agents

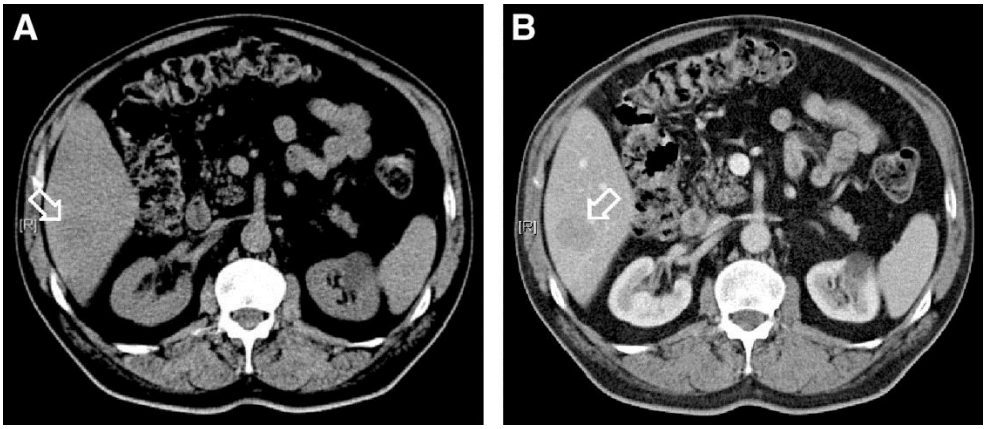

Figure 2: CT images (A) without contrast agents, and (B) with contrast agent

Since hard tissues like bone, cartilage are high in density, they absorb a great amount of X-rays, and hence produce a good contrast in the CT image. On the other hand, soft tissues like muscles or blood vessels, cannot give a similar contrast due to less radiation absorption. Consequently, minute details or defects in these tissues can be missed by the resultant compromise of image quality. This problem can be solved by 'contrast agents'. They are essential components of the imaging process for enhancing the contrast in the images obtained.

Fig. 2 shows the difference caused by injecting a contrast media in the patient's body. The contrast agent (CA) traverses through the vasculature into minor body parts and thus gives brighter images, with more clarity.

Majority of the CAs in market are iodinated organic molecules. Iodine is an element having high atomic number (Z = 53), and hence it has a high attenuation power[3]. Thus, iodinated contrast media absorb a great fraction of the X-rays incident on the body. Barium-based CAs (Z = 56) are common for Abdomen or GI tract scans[4], and are taken orally. Gold (Z = 79) is also an emerging element used for giving contrast in CT. It is generally investigated in the form of nanoparticles[5]. Gadolinium is another element which has been tested for its high contrast giving properties, due to its high atomic number (Z = 64)[3], however, it is more popular as a Magnetic Resonance Imaging (MRI) contrast agent, due to its good relaxivity[3]. All these elements are good attenuators of X-rays due to their high atomic numbers.

The common iodine-based CAs can be classified according to their ionic properties, and consequently osmolality etc. Ionic compounds have high osmolality since they undergo dissociation in solution and increase in number of moles[6]. Whereas, the nonionic CAs have low osmolality since they do not dissociate in solutions. The high osmolar CAs have greater side effects on the body, than the low osmolar. Due to the osmotic pressure created both of the high and low osmolar CAs are retained for a longer time in the kidneys than the iso-osmolar compounds[7]. Hence, they cause nephrotoxicity harming the well-functioning of the kidneys. Table 1 shows examples of high osmolar contrast media (HOCM), low osmolar contrast media (LOCM) and iso-osmolar contrast media (IOCM)[6]. The typical content of iodine in all these contrast agents is approximately 300 to 350 mg/ml.

The non-ionic CAs have proved to be a better and comparatively safer option than the ionic ones. However, they are also much more expensive than the ionic CAs[8].

Table 1 Classification of iodine-based contrast agents according to their osmolality.

Substance	Iodine content	Osmolality	Classification
Serum	-	290 mOsm/kg	-
Diatrizoate (Ionic monomer)	300 mgI/ml	1570 mOsm/kg	HOCM
Iohexol 240 (Nonionic monomer)	350 mgI/ml	518 mOsm/kg	LOCM
Iodixanol 320 (Nonionic dimer)	320 mgI/ml	290 mOsm/kg	IOCM

Since the advent of nanotechnology, there has been a leap of progress in the field of biomaterials. Nanoparticles have the property of longer retention time in the body tissues, than the molecular contrast agents. This can also help in the long-term imaging of the tissues, or for multi-modal imaging[9]. If labeled with florescent proteins or radioactive elements, these nanoparticles can be used to track molecular functions in the body[10]. Moreover, use of different types of carbon nanoparticles is booming in the biomedical industry. In the case of CAs, these carbon nanoparticles are also creating an impact with their brilliant optical properties[11-13]. One of these carbon-based materials is discussed below.

1.3 Graphene: Potential use in Contrast agents

Graphene is a 2-dimensional material, whose backbone contains sp^2- hybridized carbon structure. The carbon crystals are arranged in a honeycomb lattice structures, and they are in single-layers[14]. It was first explored by Novaselov and his group in 2004 for the study of electric field created in it[15].

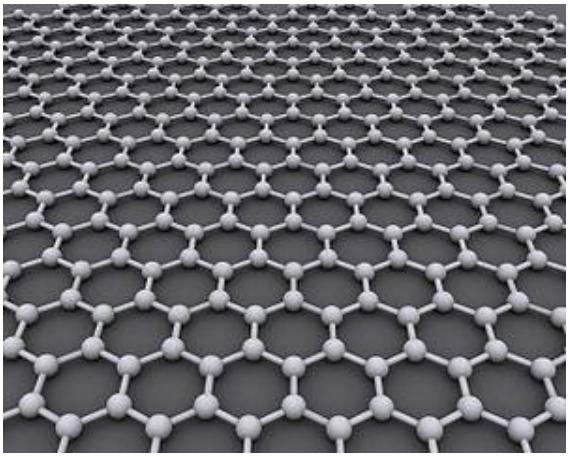

Figure 3 Schematic representation of a single layer graphene sheet16

Graphene possesses exceptional thermal, electrical, optical and mechanical properties, for which it is largely researched for a variety of applications. The opacity of graphene structure has been presented very effectively by R.R. Nair and group[17]. Besides, the biocompatible properties of graphene have triggered research in many biomedical fields[12,18-20]. Due to all these properties, we hypothesize graphene-based nanomaterial to be a good competent in the CT contrast industry.

Although it has these unique optical properties, graphene alone would not be enough to produce the desired contrast in the CT imaging because high concentrations of graphene will be needed in that case. That would possibly turn out to be harmful to the patient's body. However, looking at the ability of graphene to be easily functionalized with different chemicals, it is hypothesized that if graphene is combined with an element of high atomic weight and a high absorption factor, it would accentuate the contrast much more. For this study, we used the model element for CT imaging, iodine.

1.4 Redox Reaction of Graphite

For the incorporation of iodine in the graphene sheets, scientists have tried to dope different carbon nanoparticles by various methods of physical adsorption or chemical bonding. For the purposes of enhancing the electrical properties of carbon nanotubes, a group has successfully tried doping them by placing the carbon nanotubes in iodine vapors[21] after some chemical modification of the carbon nanotubes. Commonly, graphene films are prepared by chemical vapor deposition, and then by exposing these films to an environment where constant pressure of iodine vapors is maintained in a double zone furnace, I ions can be intercalated within the graphene sheets[22-24]. In one study, graphene was doped with iodine using camphor as the carrier substance and a carbon precursor, since camphor has a boiling point (204 °C) similar to that of iodine (184.3 °C)[25].

In our study, the purpose of iodine intercalation in graphene was to make graphene sheets as a carrier for the iodine molecules for them to go through the body. So, physical adsorption may lead to dissociation of the ions after they enter the system or when the particles are diffusing out of the vascular system. Moreover, the processing methods mentioned above involve extreme conditions of pressure and temperatures, which may incur more expenses and require careful operating measures. Production of graphene can be done by mechanical methods like exfoliating graphite particles or cleavage of highly pyrolytic graphite[26], or by chemical vapor deposition[27,28]. Oxidation and then reduction of graphite is a common chemical method of producing graphene sheets from graphite. Oxidation of graphene induces deformities in the sp^2 bonding of carbon atoms on a large scale due to the binding of oxygen atoms, which results into formation of sp^3 carbon bonds[29]. These deformities are again restored to the original sp^2 alignment of carbon

structure to some extent, when the graphene oxide is reduced by strong reducing agents[30]. The application of this method can be further extended to include the desired elements or compounds in the graphene sheets by using a suitable oxidizing or reducing agent in the redox reaction. The ions formed after the reactions using these chemicals are intercalated into the graphene sheets through strong ionic bonds.

Graphene oxide was first prepared by B. Brodie in 1859 using potassium chlorate and nitric acid as oxidizing agents[31]. Then later, a series of changes were brought about in the methods and materials used to achieve a more efficient process of oxidizing graphite[1,32]. Hummer's method is considered to be a standard procedure[33], which people use for oxidation of graphite and modify it according to their needs[34-37]. In this study, since the purpose was to incorporate iodine ions, we used Hofmann's method in which we replaced the potassium chlorate by potassium iodate.

1.5 Potassium Iodate

Potassium iodate is an ionic compound consisting of the two ions K^+ and IO_3^- in equal ratios. It is a strong oxidizing agent. The typical oxidative reactions that take place in the presence of potassium iodate can be represented as follows[38].

$$IO_3^- + 6H^+ + 6e \rightleftharpoons I^- + 3H_2O$$

$$IO_3^- + 5I^- + 6H^+ \rightleftharpoons 3I_2 + 3H_2O$$

Iodine (I_2) being an halogen like chlorine (Cl_2) and falls in the same column in the periodic table, the iodine in potassium iodate (KIO_3) is expected to have the oxidation number same as that of chlorine in potassium chlorate ($KClO_3$) during an oxidizing reaction[39]. The

Material Safety Data Sheet (MSDS) of potassium iodate describes the possible hazards and the safety measures that have to be undertaken while handling of this chemical.

1.6 Dextran

After the preparation of the reduced graphene oxide, it is observed that they do not form a stable solution in aqueous solvents. They tend to aggregate in distilled water and other inorganic solutions. In order to prevent this, the particles need to be coated with a hydrophilic compound that lends stability to the agent in a solution form. It should also be readily acceptable by the body.

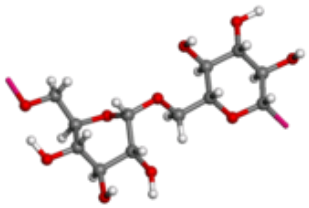

Figure 4 Structure of Dextran (http://en.wikipedia.org/wiki/File:Dextran_ball-and-stick.png)

Dextran is a hydrophilic and complex polysaccharide and has many biomedical applications[40]. It is used as an anti-thrombotic factor since it reduces the blood viscosity and it also acts a volume expander in anemia[41]. Because of its high solubility in aqueous phase, it is used to functionalize many biomaterials or nanoparticles, in specific, to improve their stability in aqueous solutions. Graphene-oxide has been coated with Dextran, in which case Dextran acts like a reducing agent on graphene-oxide[42]. Another advantage of attaching Dextran molecules to the graphene sheets, is that it provides scope to formulate a targeted delivery system[43]. The ligands of the receptors, specific to the cells of the targeted tissue, can be attached to the dextran molecules through the hydroxyl groups[44]. These functionalized particles can then travel through

the blood vessels, and get diffused into the desired tissue. This would help in driving most of the injected contrast media, to the affected tissue to be imaged and hence, preventing it from being distributed in the unwanted organs.

Thus, in this researach project, we have tried to formulate a system of Graphene NanoPlatelets (GNPs) which incorporate iodine ions by the mode of chemical reactions involving oxidation and reduction by strong iodine compounds. The experimental study design includes potassium iodate as the oxidizing agent. The efficiency of this method of synthesis is compared to that using non-iodine based oxidizing agent used by Hummer (potassium permanganate) for oxidation of graphene. In both the cases of oxidation, the graphene oxide produced was reduced by a strong iodic acid (hydrogen iodide or HI)[13,30]. To make this system more feasible for being used in a biological environment, we coated it with dextran. Then we used these dextran-functionalized particles to test its effect in vitro on cells, and also to test their contrast giving capacity while imaging.

1.7 Characterization studies:

For any biomaterial to be tested for its application, characterization of that material is very necessary in order to predict its efficiency in terms of its functionability. The requirements of a CT contrast agent in general are as follows:

1. Biocompatible material – It should not induce adverse reactions (chronic or acute)
2. Optical properties – The material should have enough absorptivity for X-rays, to produce a considerable contrast in the CT scans.

3. Iso-osmolality – To be able to flow along with the fluids in the blood vessels, the contrast media should be in the same range of osmolality, as that of the serum in the blood. High osmotic or very low osmotic can cause more side effects than the iso-osmolar contrast agents.
4. Appropriate size – The size of the material should be small enough to be able to diffuse out of the vasculature into the target tissue to be imaged.
5. Least side effects – The CA should produce least chronic or acute adverse effects on the body organs, particularly on the kidneys.
6. Proper biodistribution and safe excretion out of the body – The information on biodistribution is necessary to know if there is concentration of the material in any body part. It mainly helps in tracking the metabolism or excretion after a stipulated time in the body.

For the validation of all these properties, some preliminary studies should be carried out using different characterization techniques. Some of the characterization techniques which can be used to analyze different properties of the material are mentioned below[45]:

1.7.1 Morphological studies:

To check the size and shape of the micro/nanostructure, some of the microscopy techniques mentioned below are used. These studies are necessary to see the integrity and uniformity of the synthesized material.

a) Scanning Electron Microscopy (SEM)

b) Transmission Electron Microscopy (TEM)

c) Atomic Force Microscopy (AFM)

1.7.2 Chemical structure studies

The following spectroscopic methods help to obtain information about chemistry or the crystal structure of the sample being analyzed. It is generally based upon the different vibrations present in a chemical bond, or the emissions and absorption spectra giving out by a compound after photon irradiations.

a) Raman Spectroscopy

b) UV/Visible Spectroscopy

c) X-ray Photoelectron Spectroscopy (XPS)

d) Energy-dispersive X-ray spectroscopy (EDX)

e) X-ray Diffraction (XRD)

f) Qualitative High Performance Liquid Chromatography (HPLC)

1.7.3 Quantification studies

These studies help to quantify of certain components in the given samples, or the size distribution of the particles. This information is necessary to decide about the dosage or the formulation of the final product, and also to analyze the productivity of the synthesis process.

a) Ion Selective Electrode (ISE)

b) Dynamic Light Scattering (DLS)

c) Quantitative HPLC

d) Osmolality

1.7.4 Biocompatibility

These studies are needed to show that the material in consideration does not produce any side effects, or least effects. After being introduced in the body, they should not trigger any immune response, or harm the body tissues. Following are some of the tests carried out to evaluate the chances of occurrence of such cases.

a) Cytotoxicity

b) Immunogenicity

c) Complement activation/ RBC aggregation tests etc.

2. SYNTHESIS AND CHARACTERIZATION: METHODS

2.1 Materials used

There were mainly four steps which were followed during the whole process of the synthesis of Dextran coated-HI reduced Graphene Nanoplatelets (Dex-HI-GNPs). The materials required can be listed based on these four steps of the process as follows:

a) Pre-oxidation of Graphite flakes

Graphite flakes - Sigma Aldrich, (<45 microns) > 99.99%

Formic acid - Sigma Aldrich, ≥95%

DI water – obtained from RO filter

b) Oxidation of Graphite by modified Hummer's method

Nitric acid - J.T Baker; 69.0 - 70.0 %

Sulphuric acid – Pharmco AAPER; 95 – 98%

Potassium Permanganate – Sigma Aldrich; ≥ 99.0%

Potassium Iodate – Acros Organics; 99.4 + %; M.W. = 214

Acetone - J.T Baker; 99.5 %

c) Reduction of Graphene oxide using hydriodic acid (HI)

Hydrogen iodide (HI) – Sigma Aldrich; 57 wt% solution in H_2O, 99.95%

d) Coating of the reduced particles with dextran.

Dextran – Pharmacosmos, Technical grade T10 (M.W. = 10,000 Da)

Ammonium hydroxide – Acros Organics; 28 – 30% solution of NH_3 in water, d = 0.91

2.2 Methods

2.2.1 Pre-oxidation of Graphite flakes:

2 g of graphite flakes were taken into a round bottom flask, and 50 ml of formic acid was added to the flask. The solution was stirred for 2 h at room temperature on a magnetic stirring plate. After the stirring is completed, the solution is poured into 50 ml Falcon tubes, and centrifuged at 3000 rpm for 25 min. The supernatant is discarded and the pellet is washed by suspending it once into water, and then into acetone, and repeating the centrifuging step after each wash. The washes are required in order to remove the formic acid from the particles. This pre-treatment helps in the exfoliation of the graphite sheets, increasing the surface area for interaction with the oxidizing agents. This in turn increases the efficiency of the oxidation method[36].

2.2.2 Oxidation of Graphite:

400 mg pre-treated Graphite flakes were taken into a flask. 20 ml of nitric acid was added to the flask, and the mixture was stirred on an ice-bath for 30 min. Next, 30 ml sulfuric acid and 3 g potassium iodate were added to this mixture and the flask was transferred to an oil bath maintained at 35° C. Here, Hofmann's and Hummer's methods of Graphene oxide production are combined. The potassium iodate which is used as a catalyst is a variation from the Hummer's modified method, where potassium permanganate is used; and in the Hofmann's method where potassium chlorate is used[46]. This protocol was repeated with the use of $KMnO_4$, as in the Hummer's modified method, for comparative studies. The oxidation process was carried out for 3 h. Then the solution was let to cool down, and 150 ml DI water was added until a brown colloidal solution was obtained. The contents of the flask were poured out into Falcon tubes.

They were washed with DI water by centrifuging at 3000 rpm for 25 min, till a clear supernatant was obtained, and for every wash, the pellet was equally dispersed in the water, so that all the unwanted ions and chemicals will be washed out. All the particles were then again suspended into DI water and then dialyzed in a dialysis bag for 2 days (Fig. 5). Dialysis is needed to diffuse out all the ions and impurities formed from the acid treatments in the oxidation process.

Figure 5 Picture of the dialysis process being carried out

2.2.3 Reduction of the oxidized Graphene Particles using Hydriodic acid:

200 mg of the dried oxidized particles were dissolved in 200 ml of DI water, and this suspension was bath-sonicated for 2 h. The ultrasonication is supposed to exfoliate all the graphene sheets that have aggregated in the solution. After sonication, 2 ml of 32.1 mM HI acid was added to the solution and this mixture was stirred on a hot plate stirrer, in an oil bath which was maintained at 85 to 90° C. The flask which contains the solution is connected to a condenser, so that all the evaporating vapors will be condensed and the volume of the experiment solution will be maintained. The condenser is constantly supplied with ice cold water. This setup (Fig. 6) was let to stand overnight for 24 h. After the completion of the reaction, the temperature was let to cool down, and the 200 ml of solution was poured out into four 50 ml Falcon tubes.

These tubes were centrifuged at 3000 rpm for 20 min, the supernatant was discarded and then the pellet was washed several times with DI water by centrifuging, till the supernatant was clear. The pellet obtained after the last wash was dried in a hot oven at 60° C under vacuum, overnight.

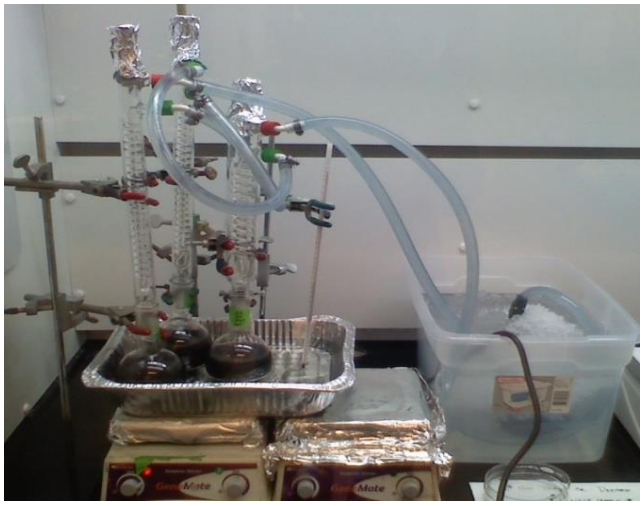

Figure 6 Picture of the reduction reaction is being carried out

2.2.4 Dextran-coating:

This step of the process was not carried out in the synthesis of first batch of HI red-GNPs. Functionalizing with dextran was mainly done to make the HI-reduced graphene nanoplatelets (HI red-GNP)s stable in solutions, and also to increase the biocompatibility of particles. For dextran coating, the flask containing 200 ml solution of HI reduced GNPs was taken as is, after the 24 h reaction set up, and bath-sonicated again for 2 hours. 2 g of dextran powder (10: 1 ratio of dextran: graphene) was added to the flask in the last 15 min of the sonication. The medium needs to be acidic for the functionalization to take place. Hence, 90 µl of ammonium hydroxide was added to the reaction flask after addition of dextran in 3 steps (30 µl at one time) at an interval of 5 min. Then the flask was transferred from the bath sonicator to the hot plate stirrer,

and the temperature was maintained at around 90° C. The mouth of the flask was again connected to a condenser as in the previous step, and the stirring was allowed to continue for 3 h. Later, the reaction mixture was made to cool down, and then poured into Falcon tubes. The tubes were centrifuged at 1000 rpm for 5 min, so that all the particles coated with dextran will remain in solution, in the supernatant, while those which are non-coated will settle down. Here, the supernatant was collected into new Falcon tubes and frozen at - 80° C. The frozen tubes were then lyophilized to give dry, dextran coated graphene nanoparticles (Dex- HI red- GNPs)

2.3 Characterization Methods

2.3.1 Raman Spectroscopy

Particles at different stages of the synthesis process, namely pre-treated graphite flakes, O-GNPs and HI-red GNPs, were dissolved into isopropanol at around 1 mg/ml concentration, and drop-casted on to silicon wafers. The ProRaman-L –Enwave was the instrument used for the spectroscopy. The CCD detector was cooled to - 52 ° C. The sample was excited with a 785nm frequency stabilized narrow line width diode excitation laser. Enwave Optronics software was used to view and retrieve the data.

2.3.2 Transmission Electron Microscopy and Scanning Electron Microscopy

Sample preparation for TEM: A solution of 1 mg/ml of the samples was made in eppendorf tubes using (1:1) DI water: ethanol mixture as solvent. The tubes were bath sonicated form 15 min, then probe sonicated for 1 min, and finally centrifuged for 5000 rpm for 5 min. 1 or 2 drops of the supernatant from each of the tube was taken and drop-casted onto 3 separate TEM grids (300-mesh size, holey lacey carbon grids (Ted Pella, USA)). The grids were set to air dry

overnight in the hood. TEM was then performed on these grids at the Center for Functional Nanomaterials (CFN) department in Brookhaven National Laboratory(NY, USA). The equipment used was JEOL 2100F high-resolution analytical transmission electron microscope.

For SEM, the HI-red GNPs were placed on a conductive, double-sided carbon adhesive tab (PELCO, Ted Pella). The SEM was performed on the JOEL 7600F Analytical high resolution SEM at the Center for Functional Nanomaterials (CFN), Brookhaven National Laboratory, NY. The samples were imaged at 5 kV using a secondary electron imaging (SEI) detector.

2.3.3 UV-Visible Spectroscopy

Concentrations ranging from 100 µg/ml to 1 mg/ml of the solutions of graphite flakes, O-GNPs and HI-red GNPs were made in aqueous solutions. A Thermo Scientific Evolution 300 UV-Vis spectrometer was used to measure the absorbance readings. VISION software was used from which we imported and analyzed the data in Excel. A reference of distilled water was used in this experiment.

To evaluate the efficiency of the dextran-coating, UV-Vis was performed using pure dextran solution as a reference on a HR 4000 spectrometer in the Material Science Engineering Department. After subtracting the absorbance of dextran from the UV-Vis spectra of the Dex-HI red GNPs, the remainder absorbance was extrapolated on the standard curve obtained for pure HI-red GNPs' solutions.

2.3.4 Atomic Force Microscopy

The samples for AFM were prepared at very low concentrations so as to prevent damage of the microscope tip. 10 µg/ml solutions of different samples were prepared in isopropanol, and drop-casted on a silicon wafer. This wafer was allowed to dry, and care was taken that the

prepared samples are covered, so that the surface may not get contaminated with other material. The Microscopy was performed using the Nanosurf Easyscan 2 Flex. The images were obtained in a tapping mode operation using a V-shaped cantilever (APP Nano ACL – 10, L = 225 µm, W = 40 µm, frequency f_c = 145–230 kHz, spring constant k = 20–95 N/m, tip radius < 10 nm).

2.3.5 Osmolality measurement

To check the osmolality of the prepared Dex-HI red GNPs, solutions of different concentrations of the lyophilized powder were prepared. The concentrations ranging from 1mg/ml to 100mg/ml were used. The instrument used to measure the osmolality of these particles was Advanced Model 3250. Cooling liquid was poured in each time, beneath the sample holder, to facilitate freezing of the sample solution.

2.3.6 Ion Selective Electrode

In order to analyze the amount of Iodine incorporated in the prepared nanoparticles, they were sent to Galbraith Laboratories (TN, USA). There, the scientists had to first extract the iodine out from the graphene sheets by a method called as Oxidative Flask Combustion. This method is typically used as a preparatory step in the determination of halogens and other elements like selenium and sulfur[47]. The apparatus consists of a heavy-walled conical flask, generally of 500 ml volume, which is fitted with a glass stopper. A test specimen carrier is fused to this stopper, which has a heavy-gauge platinum wire and a piece of welded platinum gauze. Safety measures are necessary while handling the instrument. The solid sample powder is weighed in a filter paper, and together with a fuse-strip, it is placed in the platinum gauze specimen holder. An absorbing liquid, specific for the element to be isolated, is placed in the flask. Air is flushed from the flask with a rapidly flowing stream of oxygen. After the liquid is

saturated with oxygen, the fuse-strip is ignited by appropriate methods. After combustion is complete, the liquid is ready to be processed for the further analysis.

Ion selective electrode is a transducer which converts the activity of a certain ion dissolved in a solution into an electrical potential[48]. This potential is then in turn measured by a voltmeter or pH meter. The transducer or sensor is generally an ion-specific membrane and comes with a reference electrode.

2.4 Cell toxicity studies

LDH assay and Prestoblue reagent assay were selected for the toxicity studies on cells. Human kidney cancer cells, A498, and mouse fibroblast cells, NIH-3T3, were selected for the toxicity studies. Due to the nephrotoxicity concerns of the CAs, it is essential to know about the effects of the CAs on the nephritic tissue. Studies have been reported where kidney cells are used for the cytotoxicity studies of CAs[49,50]. A human cell line was used to simulate the human body environment as far as possible. NIH 3T3 are commonly used for transfections and for cultivation of keratinocytes. Here, they were selected for their non-cancerous nature.

The A498 cells were cultured in EMEM medium, and NIH-3T3 cells were cultured in DMEM medium. The cells were seeded into 96-well BD Falcon plates with a number of $10^{\wedge 4}$ cells per well. Following day, these cells were treated with the Dextran-coated HI-red GNPs of concentration 5 mg/ml to 50 mg/ml. 50 µl of the particle solution were added to 200 µl of the culture medium in the wells, so that the final concentrations of the particles was diluted 5 times. The assays were carried out at 2 time points: 24 h and 48 h.

LDH assay: After 24 h of the particle treatment, the 96 well- plates were centrifuged at 2000 rpm for 5 min, so that all the dead cells and impurities would settle at the bottom of the wells. Then 50 µl of the media from the top of each well was pipetted out into a new 96 well-plate. 100 µl of LDH reagent (LDH substrate + dye solution + co-factor in 1:1:1 ratio) was added to the wells in the new plate. The plate was incubated for 45 min and then, the absorbance reading at a wavelength of 490 nm was recorded in a plate-reader.

Prestoblue assay: The medium from each well of the particle-treated plates was removed after the completion of the 24 h time point and 100 µl of Phosphate Buffered Saline (PBS) was added to all the wells to give them a wash. Then PBS was also removed from the wells and 100 µl of new media was added to the wells. Next, 10 µl of Prestoblue reagent was added to each well, and the plate was incubated for about 30 to 40 mins. The absorbance was measured at a wavelength of 570 nm, and the reference absorbance values were taken at 600 nm. The difference of values at these two wavelengths was taken as the final reading of the assay.

The sample size for each group of wells was taken as 8. Statistical analysis was performed on the assays in Microsoft Excel using one-way ANOVA test and the Student's t-test.

2.5 CT phantom studies

The phantom studies were performed at the Medical Center of the Stony Brook University. A General Electric (GE) CAT scanner was used to take images of the phantoms. The CT phantom is a big glass cylinder, filled with water. Essentially, it is used to validate or analyze the performance of an imaging modality and it is generally water- based. Phantoms are used in place of living things to be imaged for studies, and they are designed in such a way that they will

have optical properties similar to a real organ or tissue. The images were taken at a 120 kV and 800 mA. This dose was higher than what is usually prescribed for patients to get a good contrast of the samples.

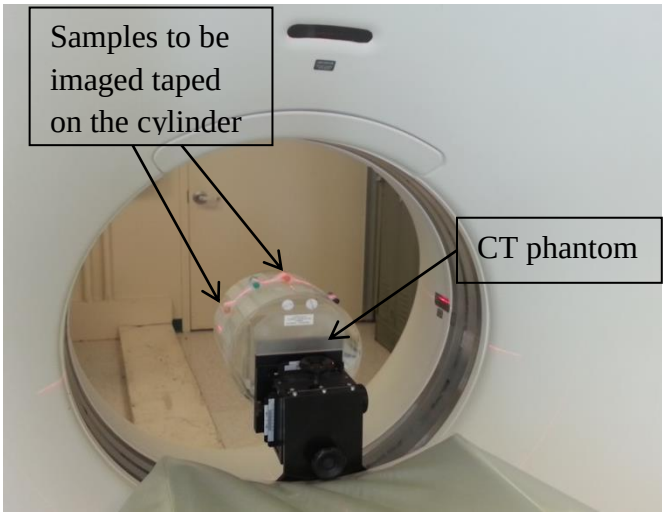

Figure 7 Picture of a CT phantom

3. Results and Discussions

3.1 Raman Spectroscopy

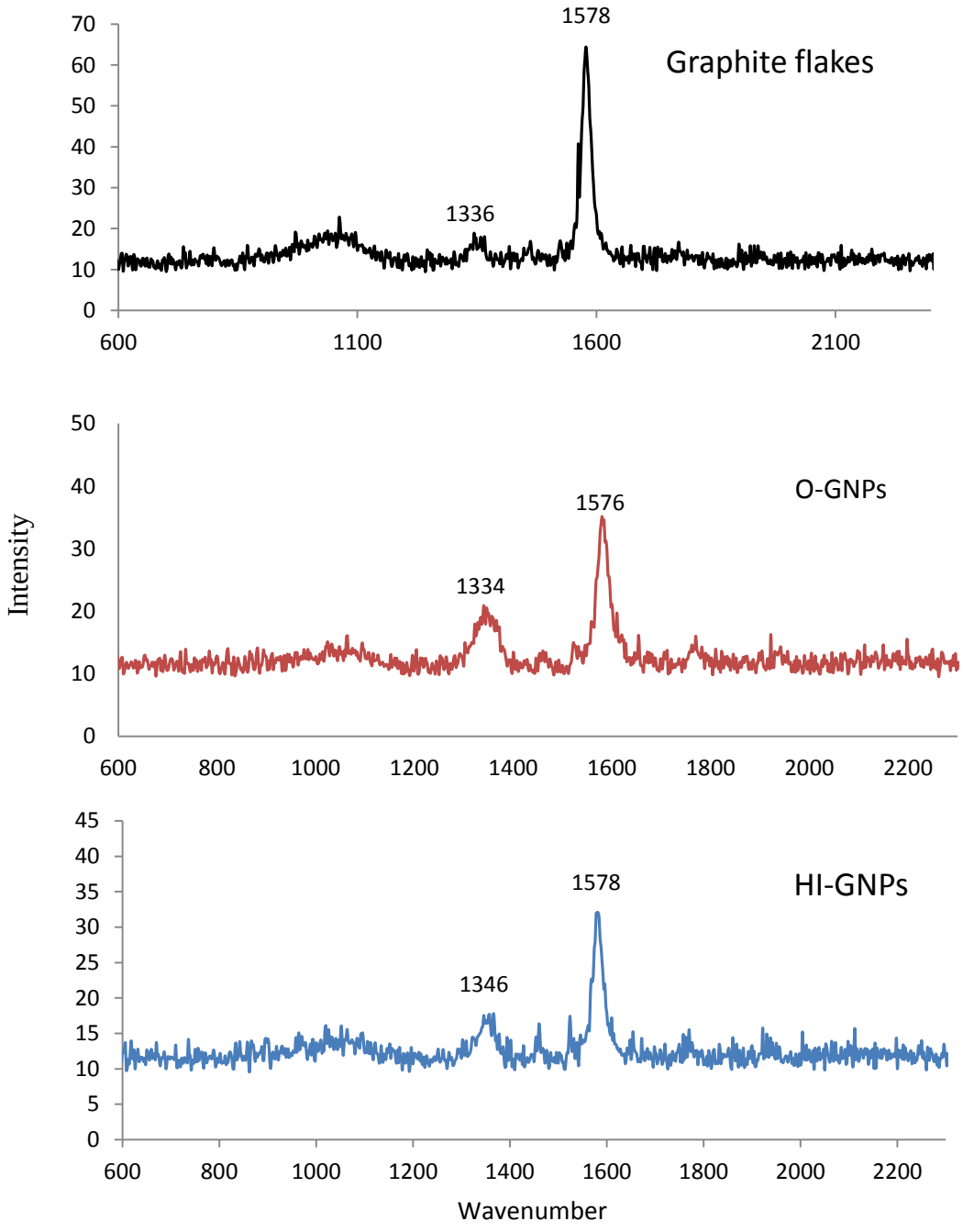

Figure 8 Raman spectra for graphite flakes (top), O-GNPs (center) and HI-red GNPs (bottom)

Raman Spectroscopy is a reliable way to detect the deformations occurring in the uniform sp^2 hybridized structure of pure graphite. Normally, a pure graphite structure gives a single peak in the spectra at ~ 1560 to1580 cm^{-1} wavenumber[46]. This peak is called as 'G band'. When deformities are introduced in this structure in the form of sp^3 hybridization, a new peak starts appearing in the Raman spectra at ~ 1350 cm^{-1} called as the 'D band'. The ratio of intensities of D band to G band (D: G ratio) gives an estimate of the extent of the deformities formed in the structure.

In the Fig. 8 above, the spectra for all the three samples are showing the G band at ~ 1577 $cm^{-1.}$ The pre-treated graphite is showing a small band at 1336, which should be due to the formic acid treatment. After oxidation, the D band is further increased in intensity due to the oxidizing deformations formed in the structure. The D: G ratio for this sample is 0.5618, and after reduction, this ratio got reduced to 0.549

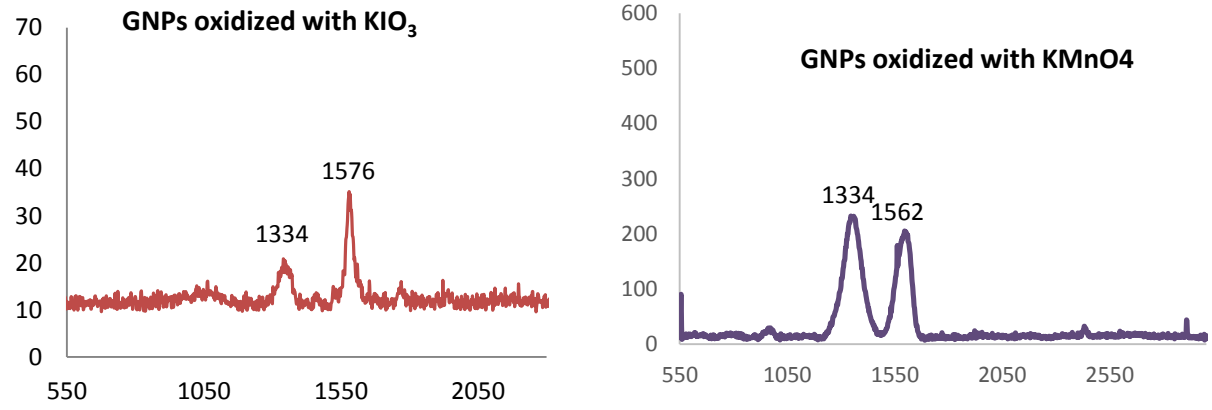

Figure 9 Raman spectra for GNPs oxidized with KIO_3 (left) and with $KMnO_4$ (right)

The Fig. 9 shows the effect of oxidization of the graphite flakes using two different oxidizing agents. The oxidized particles made using potassium permanganate are showing a much higher D: G ratio (1.169) as compared to that of the oxidized particles made using potassium iodate (0.5618). This tells us that the efficiency of $KMnO_4$ to oxidize graphite is much more than that of KIO_3. The high intensity and less noise in the spectra shown on left also prove the purity of the graphene oxide.

3.2 SEM and TEM

SEM images at different magnifications are shown in Fig. 10 are taken only for HI-red GNPs. They show a large size distribution over the range of a few hundreds of nanometers to 10 to 20 µm, and they all show a 2 dimensional sheet like structure.

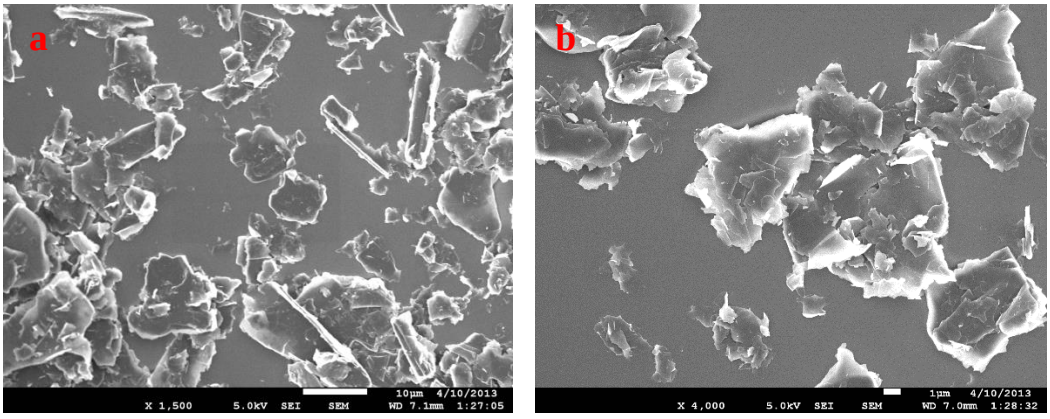

Figure 10 SEM images at a scale of 10 µm (a) and 1 µm (b)

Fig. 11 (a) below shows the TEM images of the micro-graphite flakes after pre-treatment. They are up to a size of 10 microns. It can be also seen that the graphene sheets are stacked together, due to which the image is looking darker. Oxidized GNPs can be seen in 11 (B), where the graphene sheets appear to be separated than the graphite flakes. We can see single

sheets, even folded up in one corner. 9 (C) again show the reduced GNPs. They again look stacked up as compared to the oxidized ones. Both the O-GNPs and HI-red GNPs seem to have reduced 8 to 10 times in size, but this reduction in size is less as compared to that of the standard graphene oxide particle size, which is ~ 200 nm.

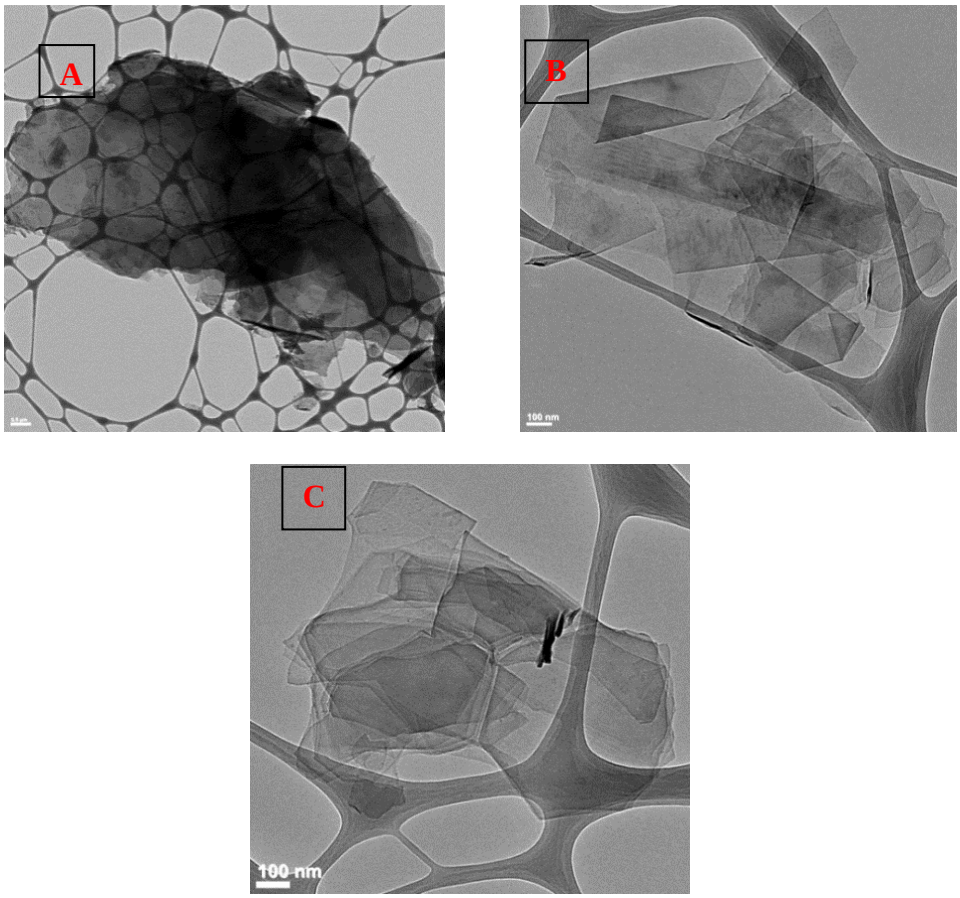

Figure 11 TEM images of the samples at different stages of synthesis: (A) Pre-treated Graphite flakes; (B) Oxidized Graphene; (C) Reduced Graphene platelets

Ideally, nanoparticles should be in the range of 100 to 500 nm, for them to be able to enter the tissue, and cells easily. But, particles which are larger than 1 micron, face a difficulty in diffusing out of the blood vessels, into the tissue and cells.

3.3 UV-Vis spectroscopy

Fig. 12 shows the UV-Vis spectra of the samples in its 3 stages of the synthesis protocol. All the spectra shown in the figure are in 200 µg/ml concentrations of the GNPs. As reported earlier, the maximum absorbance of the O-GNPs is around a wavelength of 227 nm and that for the HI-red GNPs has been red shifted to around 254 nm[51]. The pretreated graphite is showing a plane standard curve with no particular peak.

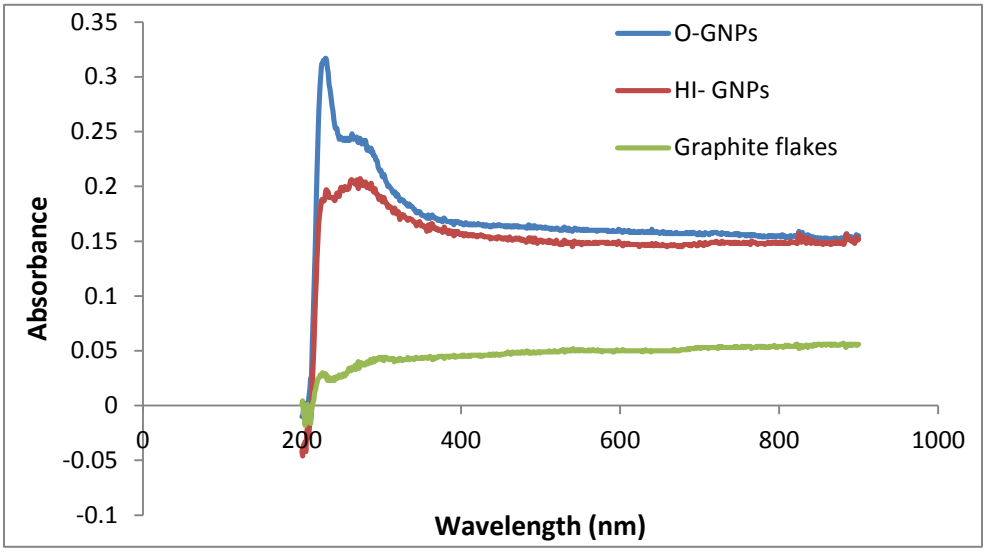

Figure 12 UV-Vis spectra of O-GNPs, HI-GNPs and pretreated graphite flakes

Dextran-coating efficiency: After dextran-coating the HI-red GNPs, it was again subjected to UV-Vis, in order to know how much of the lyophilized powder contains actual GNPs. Pure dextran solutions corresponding to the concentration of the dex-coated HI-red GNPs were used as reference solution for the observations. A standard curve was obtained for the non-coated HI-red GNPs of increasing concentrations. The readings of the dex-coated particles were then extrapolated on this standard curve. Dextran was added 10 folds of the GNPs amount during

the functionalizing step in the synthesis. According to the UV-Vis reading (Table 2), 5mg of Dex-coated GNPs contain only 257.933 µg of the HI-red GNPs. Similarly, 15 mg of Dex-coated particles contain 797.266 µg of GNPs. Hence, on average, only 52.35 % of the graphene nanoplatelets remained in the solution after the centrifugation of the dex-coating solution.

Table 2 Calculation of dextran coating efficiency from UV-Vis spectrometry data

Dex-coated GNPs	Absorbance	HI-red GNPs	Coating efficiency
5 mg/ml	0.391	257.933 µg/ml	51.6%
15 mg/ml	1.2	797.266 µg/ml	53.1%

3.4 AFM

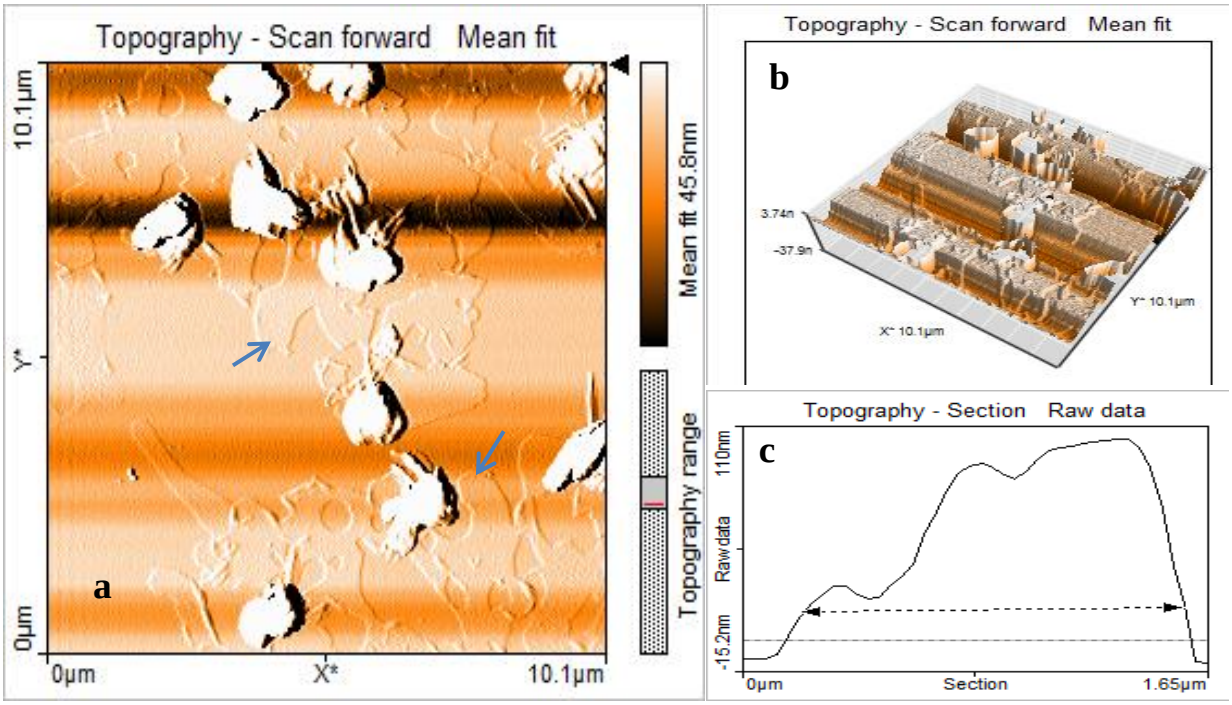

Figure 13 AFM of HI-red GNPs in a color map (a), 3-D map (b) and a cross section of one particle (c)

Fig 13 shows the AFM images of HI-red GNPs as a color map, a 3 Dimensional map with a mean fit and a line map of cross section of one the particles seen in the color image. The window scale was 10 microns. Line map of the cross-section shows that the particle is ~ 1.37 microns. The height of the cross-section shows that it is about 110 nm thick, which tells us that this might be the representation of a stack of reduced graphene sheets. Whereas, the structures pointed out by arrows in 12(a), showing considerably less contrast, have a height of only about 4 nm. That indicates the presence of single sheets of HI-red GNPs.

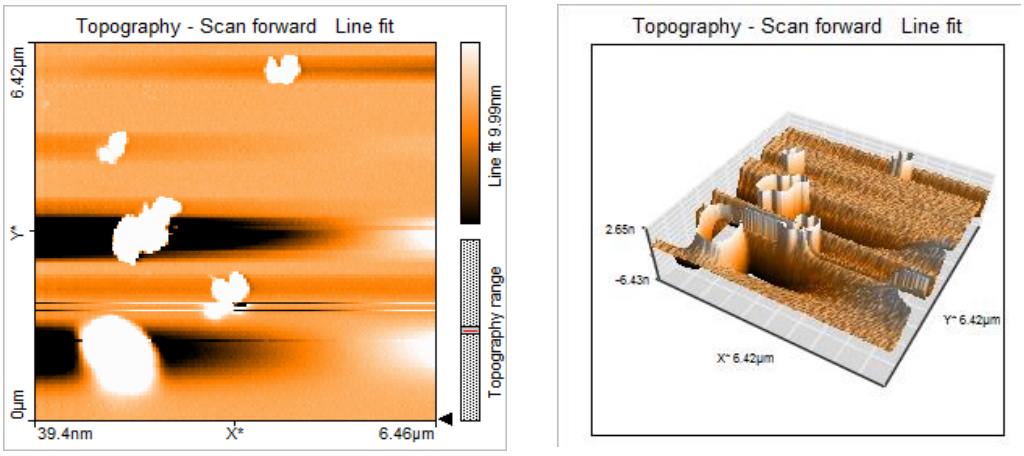

Figure 14 AFM of the O-GNPs with a line fit data.

AFM images of oxidized GNP-s are shown in Fig 14. The 3-D image shows height of the particles around 2.65 nm, and the width varying from 400 nm to 1.3 microns.

3.5 Osmolality

For the two times when this study was carried out, solutions were prepared new from the lyophilized Dex-HI red GNPs. The readings obtained both the times are considerably consistent (Table 3). The 100 mg/ml solution showed an osmolality of average 36 milliosmoles. This is

quite low than that of the serum. If injected as is, it would cause hypo-osmotic pressure in the blood system, which would lead to eruption of the blood cells due to excessive inflow of solvent into them. Consequently, it becomes necessary to compliment the solution to increase the osmolality of the contrast agent up to that of the serum (290 mOsm). The possible solutions are discussed in the next chapter.

Table 3 Osmolality readings of the Dex-coated samples

Concentrations (mg/ml)	1st Readings (mOsm)	2nd Readings (mOsm)
1	1	0
10	5	5
25	11	8
50	21	22
75	24	27
100	37	35

3.6 ISE analysis

The results from Galbraith Labs showed the amount of Iodine present in the 5 samples. Oxidized and reduced GNPs prepared in two batches were given to check for the reproducibility of the synthesis process. The iodine content was expressed in parts per million as shown in Table 4. The contrast produced by the GNPs has to be comparable to the iodinated contrast agents, whose iodine content is around 300 mg/ml (refer to Table 1) The concentration of iodine obtained in this study (highest being 6309 ppm) was considerably low than expected[13]. As was hypothesized, some of the iodine was incorporated during the oxidation step of the synthesis using potassium iodate, and this amount increased during the reduction of the GNPs with HI. The increase in the iodine content is consistent with both the batches of synthesis of HI-red

GNPs, however, the amount incorporated in the GNPs is significantly variable for the two batches (168 ppm and 743 ppm). The high iodine content in the Dex-HI-red GNPs is seen because of the trapped iodine in the dextran solution. This is an experimental error as the extra iodine is not intercalated into graphene sheets. Once they are dissolved in solution, these iodine ions will be directly dissolved in water, rather than being trapped in the platelets.

Table 4 Results showing the Iodine content in different samples in parts per millions

Sample description	Sample Amount Used	Iodine content (ppm)
Batch 1-oxidized graphene platelets	29.93 mg	124
Batch 1-HI-reduced graphene platelets	28.89 mg	168
Batch 2-oxidized graphene platelets	34.41 mg	562
Batch 2-HI-reduced graphene platelets	14.20 mg	743
Batch 2-Dextran coated-Hi reduced graphene platelets	31.49 mg	6309

3.7 Cytotoxicity studies

LDH assay: It is a dead cells based assay. The LDH assay works on the principle of measuring colorimetric product formation after an enzymatic reaction. Essentially, enzyme lactose dehydrogenase (LDH), which is a cytosolic enzyme, is released from the damaged plasma membranes after cell death. This released LDH is coupled to an enzymatic reaction, at the end of which a red formazan product is formed. This red formazan compound, which is

directly proportional to the amount of LDH released, is then quantified by measuring the absorbance at a wavelength of 490 nm.

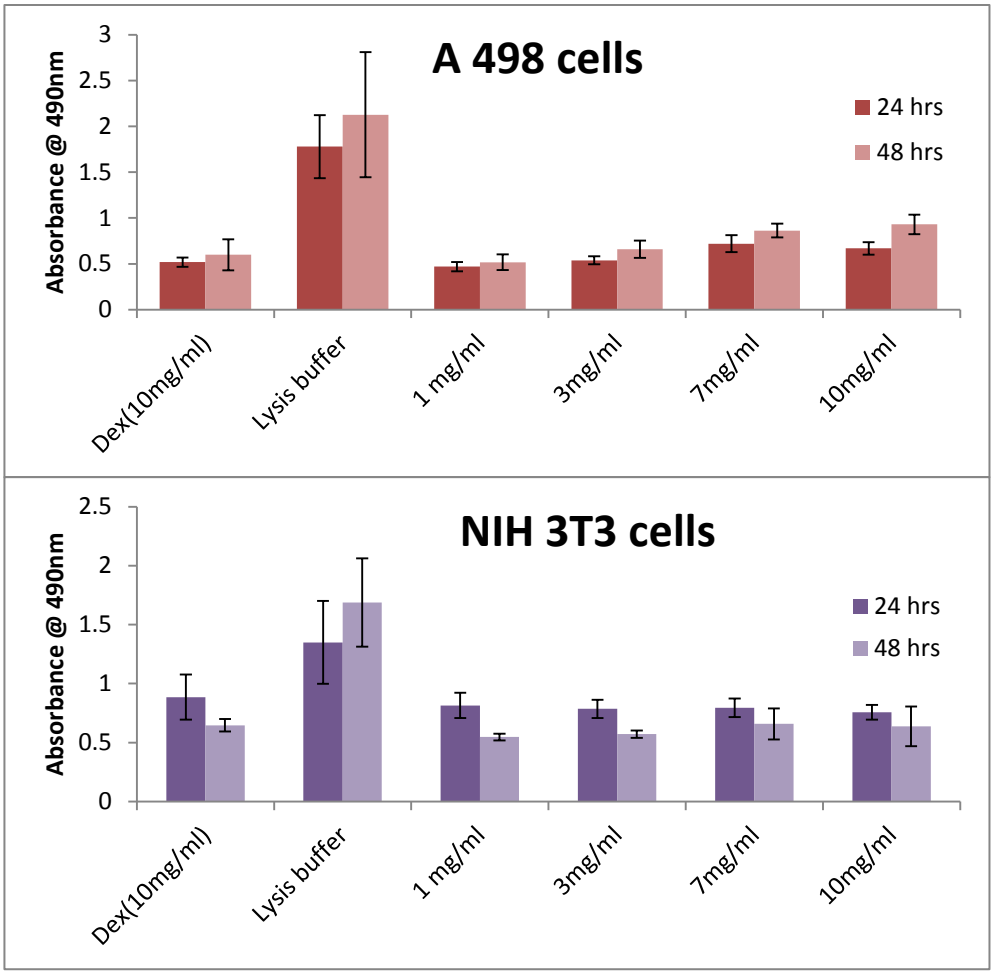

Figure 15 LDH assay measurement for A498 and NIH 3T3 cells, at 24 h and 48 h time point.

We can see from Fig. 15 that for the A498 cells, the cell death has increased with increasing concentrations of the Dex-coated particles from 1 mg/ml to 7 mg/ml. The absorbance for the two highest concentrations in case of both the cell lines, is not significantly different. However, the ANOVA test showed that the variation of the absorbance for the increasing concentrations of the particles is significant.

For the NIH3T3 cell line, the cell death occured was not found to be significantly different for the increasing concentrations for both the 24 and 48 h time points. For both the cell lines, the maximum cell death occurred after 48 h by the Dex-HI red GNPs treatment is less than 50% of the total dead cells which was used as a positive control. So, we can generalize that the cytotoxicity of the dex-coated particles is not significant even at high concentrations. This is in accordance with previously published data about the graphene toxicity[40,52]. 10 mg/ml Dextran solution was used as a control for the Dex-coated particles. It showed a certain toxicity of its own, which was more than the least concentrated HI-red GNPs solutions.

Prestoblue assay: This is a live cell assay. The presto blue reagent is a resazurin-based solution which is cell-permeable, and it is quickly reduced by the metabolically active cells in the wells. For measuring absorbance, incubation time of 20- 30 min was used and the measurement wavelength was 570 nm, with 600 nm as the reference wavelength.

Fig. 16 is showing the results for the viability of both the cell lines at 2 time points using this reagent. For the A498 cells, the plot is showing decreasing cell viability for an increasing particle concentration for the first 24 h. This is a statistically significant variation in the cell viability ($p < 0.05$). However, the viability is showing the opposite trend after 48 h. Moreover, the data does not show a significant difference for the 48 h time point. The difference in the absorbance values for the fibroblast cells are also found to be insignificant ($p > 0.05$) and lead to no certain trend line of the cell viability.

The ambiguity of these results may be due to the interference of the remaining particles after the PBS wash, with the absorbance at the measured wavelength.

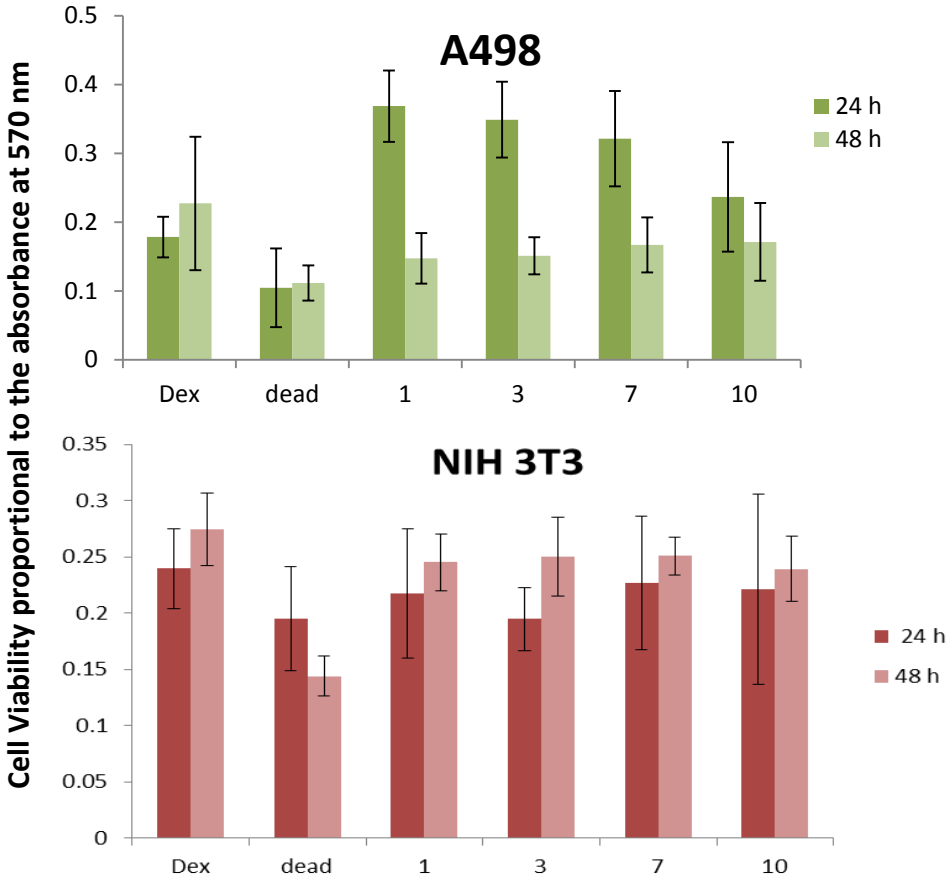

Figure 16 Prestoblue assay results for A498 and NIH 3T3 cells at 24 h and 48 h time point

Overall, the A498 cells appear to be more sensitive to the concentrations of the Dex-particles than the NIH 3T3 cells, which is indicated by both the live and dead cell assays. This may be because the former being a cancer cell line, is more sensitive to the changes in its environment. On the other hand, the latter cell line (fibroblasts) must be robust enough to survive even at high concentrations of the functionalized nanoparticles. Moreover, after 48 h, the A498 cells show a decrease in proliferation, whereas the fibroblasts show an increase. This verifies the assumption that the particles have less effect on the fibroblasts viability than on the A498 cells.

Comparative analysis of cytotoxicity of two different particles: To compare the cytotoxicity of particles produced by the oxidation with $KMnO_4$ and those produced by oxidation with KIO_3, LDH assay was performed on the two cell lines using equal concentrations of both the particles. The absorbance which the cells showed for the positive control (dead cells) differed since the assay was performed in two different weeks for two different set of particles. In order

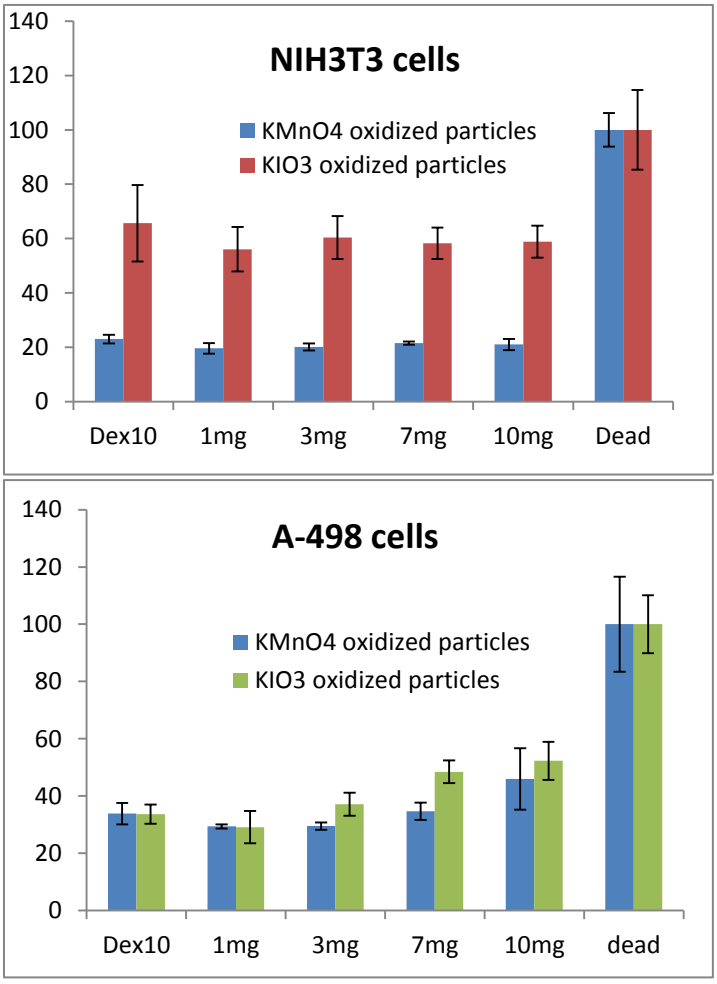

Figure 17 Comparative results for LDH assay treated with particles oxidized with $KMnO_4$ and KIO_3.

to be able to compare the effects of the particles on cells, with the same basis, the absorbance of all other samples was expressed as a percentage absorbance of the positive control.

The resulting data analysis (fig. 17) verifies that the KIO_3 oxidized particles are more toxic to the fibroblasts (NIH3T3 cells) than the KMnO4 oxidized particles. T-test was performed in Microsoft Excel to check the significance of the difference of toxicity. The p-value for the NIH 3T3 cells came out to be 2.693e-06 and that for the A498 cells was 0.3409. Hence, the toxicity of the KIO_3 oxidized particles on the A498 cells was not significantly different from the KMnO4 oxidized particles. However, it was significantly higher for the fibroblast cells than for the KIO_3 oxidized toxicity.

3.8 CT phantom studies

For the first round of the phantom studies, several concentrations of the HI (8 mM, 16 mM, 24 mM and 32 mM) were taken as controls along with two experimental sets of varying concentrations of Dex-HI red GNPs, maximum being 45 mg/ml. One set was of the particles prepared using KIO3 and other was the one using KMnO4. However, since the iodine content was very less even in 45 mg/ml of the solution, the contrast obtained was not enough to be able to compare with the 32 mM HI solution (see Fig. 18). Yet, comparatively, the 3 samples which have KMnO4 oxidized Dex-HI-red GNPs (shown by thin arrows) exhibit a slightly more contrast than the KIO3 oxidized Dex-HI-red GNPs samples (shown by block arrows). This can mean that the KMnO4 oxidized GNPs contains more iodine than the other set of particles.

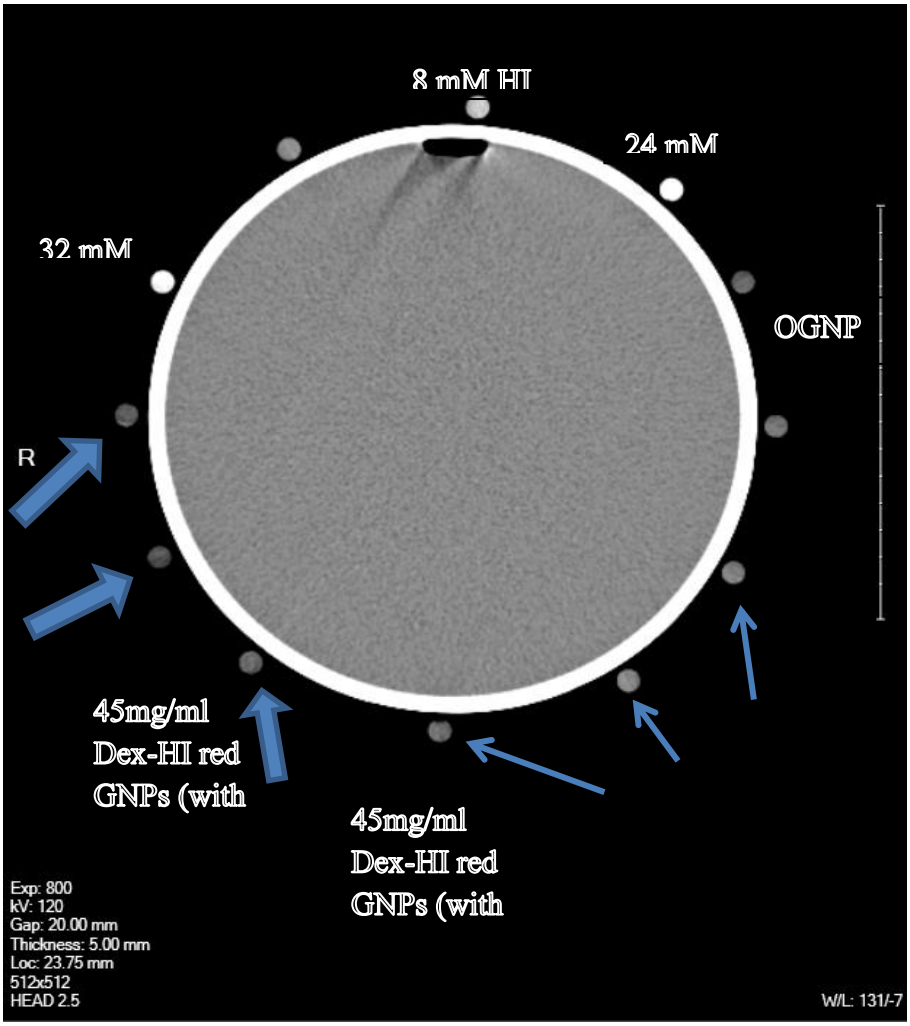

Figure 18 CT phantom image of the 12 samples (first round)

In the second round of phantom study, Dex-HI red GNPs were taken in a concentration equivalent to 1 mg of Iodine per ml. This concentration was found to be approximately about 160 mg of the Dex-HI red GNPs per ml of water, from the ISE results shown before.

The phantom image for the second round of the study is shown in Fig 19. Five tubes were taken for this round. 3 of them were HI acid of concentrations 4 mM, 8 mM and 16 mM (Circles 1, 2 and 3 respectively in Fig. 19). The 8 mM tube contained approximately 1 mg/ml of iodine,

and Dex-HI-red GNP solution of 160 mg/ml which contained approximately the same amount of iodine was taken, so that comparison between the contrast produced will be easy.

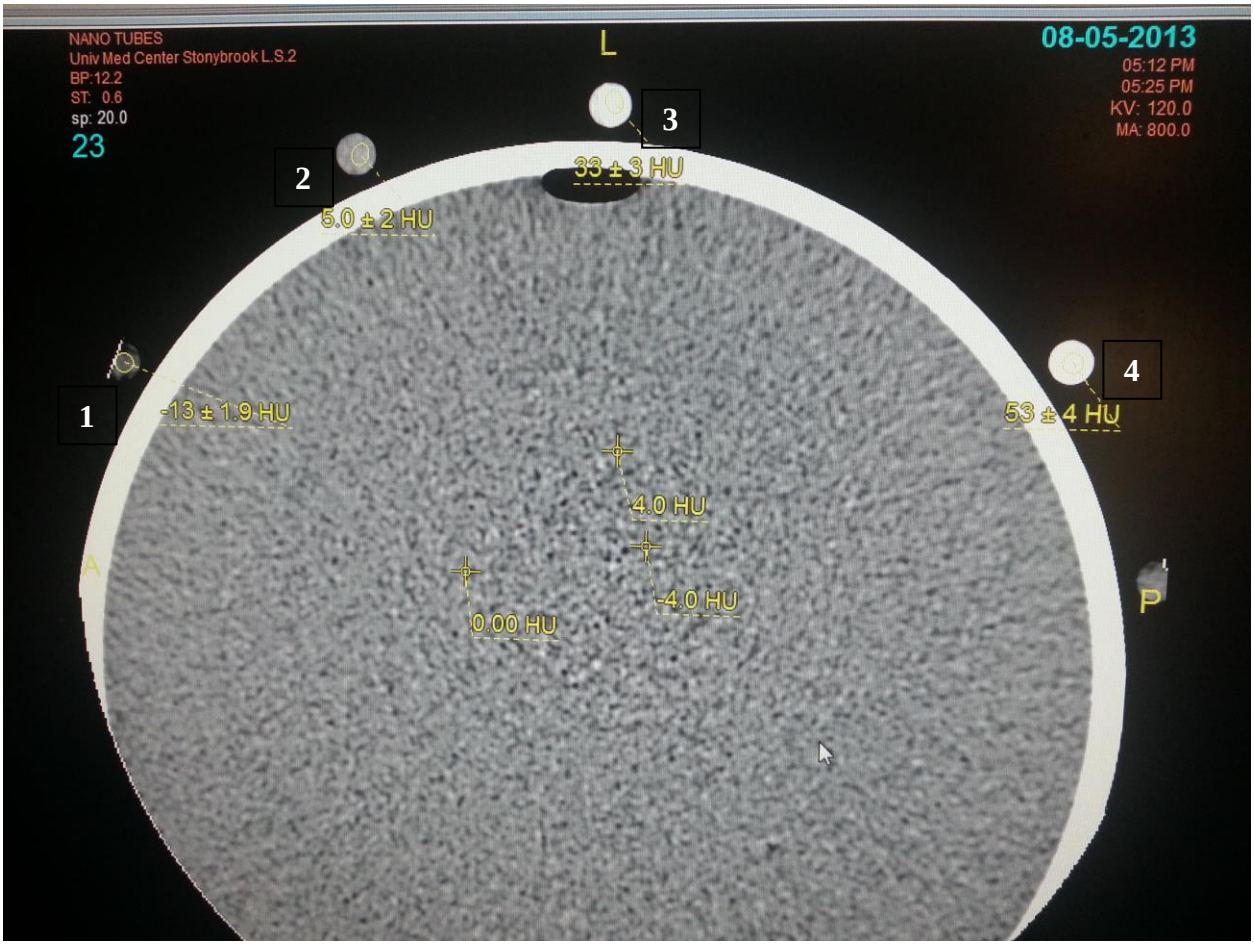

Figure 19 CT phantom image with experiment sample containing approximately 1 mg iodine

The contrast of the samples shown in the figure above is measured in Hounsfield Units (HU) which specifies the linear attenuation coefficient measurement of the object (μ_x), relative to that of distilled water (μ_{water}), as shown by the following equation.

$$HU = 1000 \times \frac{\mu_X - \mu_{water}}{\mu_{water}}$$

CT scanners use this unit to calibrate the instrument with reference to water. Here, the HU numbers were obtained for the different concentrations of HI (Fig. 19) in the second round of imaging studies. These numbers are plotted against the iodine content of the same solutions. A linear relation is observed after plotting the graph as shown in Fig. 20.

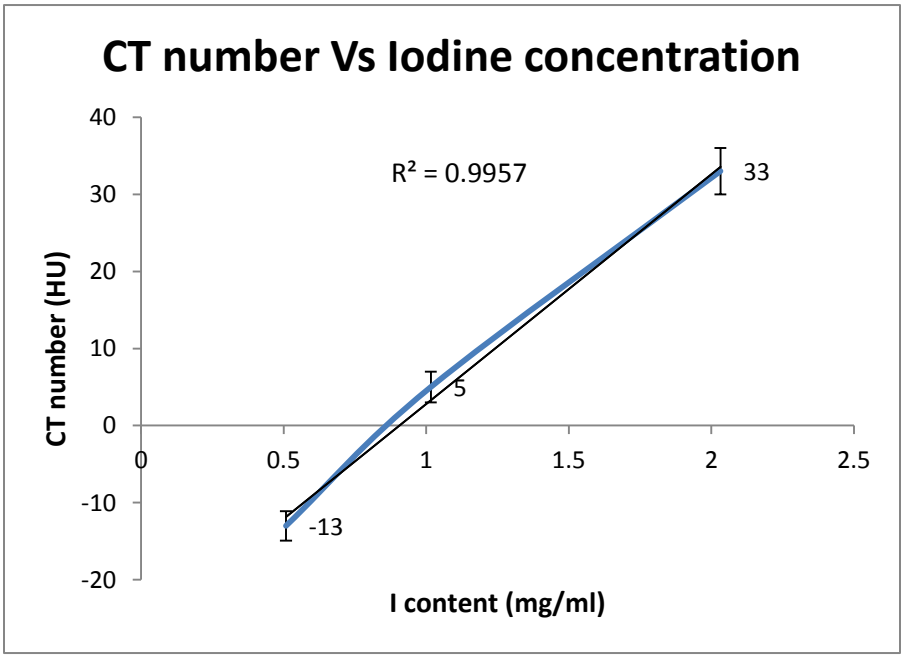

Figure 20 Relation of HU to the concentration of Iodine

The CT number for the experimental sample of Dex-HI-red GNP was found to be 53 ± 4 HU. Consequently, the graphene platelets incorporating iodine prove to have a better attenuation co-efficient, and hence a better contrast than a pure HI solution having equivalent amount of iodine present in it.

In order to get an idea of the relative contrast produced by these particles, we can compare them with actual Hounsfield Units. Table 5 shows the standard values of these CT numbers which are obtained for actual organs and substances in the body. We can see that the bone has much larger attenuation co-efficient than other substances or soft tissues in the body.

Table 5 Hounsfield Units for common substances[53]

Substance	HU
Air	−1000
Lung	−700
Soft Tissue	−300 to -100
Fat	−84
Water	0
CSF	15
Blood	+30 to +45
Muscle	+40
Bone	+700(cancellous bone)to +3000 (dense bone)

When compared to the results obtained from the experiments in the current research work, we can say that the contrast obtained is still in the range of certain soft tissues like muscles or blood. This shows the lack of iodine in the Graphene platelets. In order to bring about more contrast in these tissues, we need GNPs with larger amounts of iodine intercalated in them. This concern is addressed in the next chapter.

4. CONCLUSIONS AND FUTURE PROSPECTS

4.1 Conclusions

This work being an open-ended research, the use of potassium iodate was not expected to show better results than the potassium permanganate, which has already been studied[11,13]. The Raman and UV-vis data do show that the graphite has been oxidized when potassium iodate was used and then reduced with HI acid. However, when compared with the Raman spectra of the GNPs oxidized with $KMnO_4$, we come to know that the efficiency of the oxidation step is considerably low when potassium iodate is used.

The results obtained by Ion Selective Electrode method somewhat confirmed our hypothesis that the oxidation step will help to incorporate the iodine in the graphene sheets, and the reduction will further add to the content. Nonetheless, the amount of content which they exhibited are too low, to consider this process as an efficient one. In this case, the dose to be injected will have to be very high which can be toxic to the body. We saw in the cytotoxicity assays that concentrations as high as 10 mg/ml also are not very toxic to the cells. Moreover, they affect the sensitive human kidney cancerous cells more than the robust mouse fibroblasts. It is evident that the toxicity of the dex-coated particles is comparable to pure dextran solutions.

Lastly, all the microscopy images show that the particle size range between a few hundreds of nanometers up to 10 microns. Having discussed the issue of large size of the particles, modifications in the synthesis step are needed in order to reduce the particle size. Increasing the time of sonication, or subjecting the graphite particles to bath sonication for around two hours in the pre-oxidation step instead of magnetic stirring can help in exfoliating the

particles more. This would lead to increase in the extent of oxidation, and reduction, which could break the particles into smaller sizes, due to the defects created in them.

4.2 Feasibility of the Dextran coated HI-reduced Graphene Nanoparticles as CT contrast media

It is evident from the CT phantom studies that the graphene in itself has considerably good optical properties. However, as discussed in the conclusion, there is still a lot of scope to modify the synthesis protocol, in order to obtain optimum amount of iodine intercalated in the graphene nanoplatelets in an easy and harmless manner.

The osmolality of these particles is shown to be much less (~35 mOsm for 100 mg/ml solution) than what is required for an iso-osmolar agent (290 mOsm). However, it complies with the data which has already been studied for the same kind of particles[54]. The solution to this can be the addition of another bio-inactive material which has considerable osmolality to complement to that of the Dex-HI-red GNPs. In the earlier mentioned study, the GNPs were mixed with a solution for mannitol, , which is an osmotic diuretic agent, to make the whole solution iso-osmolar. These particles are proposed to be used as contrast agents in MRI.

With a number of adverse effects seen in case of the iodine-based contrast agents, and looking at the high costs of the less harmful or non-ionic contrast agents, we can look at some economical and affordable material which can be easily synthesized, and has minimal or lesser side effects. Graphene-based Contrast agents can be a good fit, given for the good optical properties and biocompatibility of this material. This work puts forward the idea about graphene incorporating iodine as a potential contrast agent. The process of synthesis has to be modified in

terms of the chemicals used, as well as the parameters set during the process. More comparative studies including characterization of chemical structure needs to be done so as to evaluate the efficiency of various protocols.

4.3 Significance and Impact

In summary, even though this work does not sufficiently provide proof of the improved iodine incorporation inside graphene, it opens many doors for further research on the iodinating graphene oxide nanoplatelets for use as CT contrast agents. After the optimization of the synthesis protocol, we believe that the Dex-HI red-GNPs would be ideal material for contrast agents. We have seen that the contrast of iodinated contrast agents is more than 10 times of the plain HI solution with equivalent Iodine content. This study also shows that the toxic effects of the Dex-HI red-GNPs on the cell cultures is within limits and is affects the robust cells less than the cancer cells. Further animal studies can be done to investigate the biodistribution of these nanoplatelets within different body organs. Its toxicity to these organs can also be evaluated in the same studies.

The Dex-HI red-GNPs can also be customized according to case-specific needs. Since the osmolality is considerably less than that of the serum, it can be modulated by the addition of mannitol[54]. In contrast to the molecular iodine-based CAs, targeted delivery of these Dex-HI red-GNPs is also possible, as discussed before. They can also be studied for multi-modal imaging due to their property of having longer retention times. Efforts need to be made in future to make the Dex-HI red-GNPs suitable to the FDA regulations and requirements. We believe that these proposed graphene-based nanoparticles will form a class of contrast agents competent to the conventional iodine-based molecular CAs.

Bibliography

1 Hofmann, U. & Rudorff, W. The formation of salts from graphite by strong acids. *Transactions of the Faraday Society* 34, 1017-1021, doi:10.1039/tf9383401017 (1938).

2 *Computed Tomography Equipment Technology Manufacturer - Analogic*, <http://www.analogic.com/products-medical-computer-tomography.htm> (

3 Gierada, D. S. & Bae, K. T. Gadolinium as a CT Contrast Agent: Assessment in a Porcine Model. *Radiology* 210, 829-834 (1999).

4 Coscina, W. F. *et al.* Gastrointestinal tract focal mass lesions: role of CT and barium evaluations. *Radiology* 158, 581-587 (1986).

5 Xi, D. *et al.* Gold nanoparticles as computerized tomography (CT) contrast agents. *RSC Advances* 2, 12515-12524, doi:10.1039/c2ra21263c (2012).

6 Robbins, J. B. & Pozniak, M. A. *Contrast Media Tutorial*. (2010).

7 Briguori, C. *et al.* Nephrotoxicity of low-osmolality versus iso-osmolality contrast agents: impact of N-acetylcysteine. *Kidney international* 68, 2250-2255, doi:10.1111/j.1523-1755.2005.00683.x (2005).

8 Bontranger, Lampignano, K. L. & P, J. *UC San Francisco Guidelines on the Administration of Intravenous Iodinated Contrast Media*. (Elsevier Mosby, 2005).

9 Pramanik, M., Swierczewska, M., Green, D., Sitharaman, B. & Wang, L. V. Single-walled carbon nanotubes as a multimodal-thermoacoustic and photoacoustic-contrast agent. *Journal of Biomedical Optics* 14, doi:10.1117/1.3147407 (2009).

10 Vasquez, K. O., Casavant, C. & Peterson, J. D. Quantitative Whole Body Biodistribution of Fluorescent-Labeled Agents by Non-Invasive Tomographic Imaging. *PloS one* 6, e20594, doi:10.1371/journal.pone.0020594 (2011).

11 Kissell, K. R. & J, W. L. *Preparation of iodine SWNTs and iodine US-tubes: Synthesis and spectroscopic characterization of iodine-loaded SWNTs for computed-tomography molecular imaging.*, Rice University Dissertation.

12 Bhavna, S. P., Barry, D. J., Shruti, K., Leonard Deepak, F. & Balaji, S. Physicochemical Characterization, and Relaxometry Studies of Micro-Graphite Oxide, Graphene Nanoplatelets, and Nanoribbons. *PloS one* 7, doi:10.1371/journal.pone.0038185 (2012).

13 Sundararaj, J. L. *Synthesis and Characterization of Iodine laden Graphene Nano Platelets via reduction of Graphene Oxide Using Hydrogen Iodide* Masters of Science thesis, Stony Brook University, (2012).

14 Chang, H. & Wu, H. Graphene-Based Nanomaterials: Synthesis, Properties, and Optical and Optoelectronic Applications. *Advanced Functional Materials* 23, 1984-1997, doi:10.1002/adfm.201202460 (2013).

15 Novoselov, K. S. *et al.* Electric field effect in atomically thin carbon films. *Science* 306, 666-669, doi:10.1126/science.1102896 (2004).

16 *Graphene*, <http://upload.wikimedia.org/wikipedia/commons/thumb/9/9e/Graphen.jpg/300px-Graphen.jpg> (

17 Nair, R. R. *et al.* Fine Structure Constant Defines Visual Transparency of Graphene. *Science* 320, 1308, doi:10.1126/science.1156965 (2008).

18 Yang, X. *et al.* Superparamagnetic graphene oxide-Fe3O4 nanoparticles hybrid for controlled targeted drug carriers. *Journal of Materials Chemistry* 19, 2710-2714, doi:10.1039/b821416f (2009).
19 Mullick Chowdhury, S. *et al.* Cell specific cytotoxicity and uptake of graphene nanoribbons. *Biomaterials* 34, 283-293, doi:10.1016/j.biomaterials.2012.09.057 (2013).
20 Singh, S. K. *et al.* Thrombus inducing property of atomically thin graphene oxide sheets. *ACS Nano* 5, 4987-4996, doi:10.1021/nn201092p (2011).
21 Zhao, Y., Wei, J., Vajtai, R., Ajayan, P. M. & Barrera, E. V. Iodine doped carbon nanotube cables exceeding specific electrical conductivity of metals. *Sci. Rep.* 1, doi:http://www.nature.com/srep/2011/110906/srep00083/abs/srep00083.html#supplementary-information (2011).
22 Jung, N. *et al.* Charge Transfer Chemical Doping of Few Layer Graphenes: Charge Distribution and Band Gap Formation. *Nano Letters* 9, 4133-4137, doi:10.1021/nl902362q (2009).
23 Kumari, L., Prasad, V. & Subramanyam, S. V. Effect of iodine incorporation on the electrical properties of amorphous conducting carbon films. *Carbon* 41, 1841-1846, doi:http://dx.doi.org/10.1016/S0008-6223(03)00172-6 (2003).
24 Omer, A. M. M., Adhikari, S., Adhikary, S., Uchida, H. & Umeno, M. Photovoltaic characteristics of postdeposition iodine-doped amorphous carbon films by microwave surface wave plasma chemical vapor deposition. *Applied Physics Letters* 87, 161912-161913 (2005).
25 Kalita, G., Wakita, K., Takahashi, M. & Umeno, M. Iodine doping in solid precursor-based CVD growth graphene film. *Journal of Materials Chemistry* 21, 15209-15213, doi:10.1039/c1jm13268g (2011).
26 Geim, A. K. Graphene: status and prospects. *Science* 324, 1530-1534, doi:10.1126/science.1158877 (2009).
27 Kim, K. S. *et al.* Large-scale pattern growth of graphene films for stretchable transparent electrodes. *Nature* 457, 706-710, doi:10.1038/nature07719 (2009).
28 Somani, P. R., Somani, S. P. & Umeno, M. Planer nano-graphenes from camphor by CVD. *Chemical Physics Letters* 430, 56-59, doi:http://dx.doi.org/10.1016/j.cplett.2006.06.081 (2006).
29 Mkhoyan, K. A. *et al.* Atomic and Electronic Structure of Graphene-Oxide. *Nano Letters* 9, 1058-1063, doi:10.1021/nl8034256 (2009).
30 He, H., Klinowski, J., Forster, M. & Lerf, A. A new structural model for graphite oxide. *Chemical Physics Letters* 287, 53-56, doi:http://dx.doi.org/10.1016/S0009-2614(98)00144-4 (1998).
31 Brodie, B. C. On the Atomic Weight of Graphite. *Philosophical Transactions of the Royal Society of London* 149:, 249-259, doi:10.1098/rstl.1859.0013 (1859).
32 Staudenmaier, L. Vol. 37 (The American Electrochemical Society, 1898 and 1899).
33 Hummers, W. S. & Offeman, R. E. Preparation of Graphitic Oxide. *Journal of the American Chemical Society* 80, 1339-1339, doi:10.1021/ja01539a017 (1958).
34 Lerf, A., He, H., Forster, M. & Klinowski, J. Structure of Graphite Oxide Revisited‖. *The Journal of Physical Chemistry B* 102, 4477-4482, doi:10.1021/jp9731821 (1998).
35 Marcano, D. C. *et al.* Improved Synthesis of Graphene Oxide. *ACS Nano* 4, 4806-4814, doi:10.1021/nn1006368 (2010).
36 Geng, Y., Wang, S. J. & Kim, J. K. Preparation of graphite nanoplatelets and graphene sheets. *Journal of colloid and interface science* 336, 592-598, doi:10.1016/j.jcis.2009.04.005 (2009).
37 Meng, L.-Y. & Park, S.-J. Preparation and Characterization of Reduced Graphene Nanosheets via Pre-exfoliation of Graphite Flakes.

38 Miller, C. O. & Furman, N. H. The Use of Iodine and of Potassium Iodate as Volumetric Oxidizing Agents in Solutions Containing Mercuric Salts. II. The Oxidation of Phenylhydrazine and of Semicarbazide by Means of Potassium Iodate. *Journal of the American Chemical Society* 59, 161-164, doi:10.1021/ja01280a039 (1937).
39 Helmenstine, A. M. *Rules for Assigning Oxidation Numbers: Redox Reactions and Electrochemistry*, <http://chemistry.about.com/od/generalchemistry/a/oxidationno.htm> (
40 Zhang, S., Yang, K., Feng, L. & Liu, Z. In vitro and in vivo behaviors of dextran functionalized graphene. *Carbon* 49, 4040-4049, doi:http://dx.doi.org/10.1016/j.carbon.2011.05.056 (2011).
41 Lewis, S. L. *Medical-Surgical Nursing: Assessment and Management of Clinical Problems*. (Elsevier Science Health Science Division, 2010).
42 Kim, Y.-K., Kim, M.-H. & Min, D.-H. Biocompatible reduced graphene oxide prepared by using dextran as a multifunctional reducing agent. *Chemical Communications* 47, 3195-3197, doi:10.1039/c0cc05005a (2011).
43 Tassa, C., Shaw, S. Y. & Weissleder, R. Dextran-coated iron oxide nanoparticles: a versatile platform for targeted molecular imaging, molecular diagnostics, and therapy. *Accounts of chemical research* 44, 842-852, doi:10.1021/ar200084x (2011).
44 Mehvar, R. Dextrans for targeted and sustained delivery of therapeutic and imaging agents. *Journal of controlled release : official journal of the Controlled Release Society* 69, 1-25 (2000).
45 Love, S. A., Maurer-Jones, M. A., Thompson, J. W., Lin, Y.-S. & Haynes, C. L. Assessing Nanoparticle Toxicity. *Annual Review of Analytical Chemistry* 5, 181-205, doi:doi:10.1146/annurev-anchem-062011-143134 (2012).
46 Poh, H. L. *et al.* Graphenes prepared by Staudenmaier, Hofmann and Hummers methods with consequent thermal exfoliation exhibit very different electrochemical properties. *Nanoscale* 4, 3515-3522, doi:10.1039/c2nr30490b (2012).
47 Horacio N. Pappa, P. D. (ed USP30–NF25) 191.
48 Lindner, R. P. B. a. E. Recommendations for nomenclature of ionselective electrodes. *Pure Appl. Chem.* 66, 2527-2536, doi:10.1351/pac199466122527 (1994).
49 Haller, C. & Hizoh, I. The cytotoxicity of iodinated radiocontrast agents on renal cells in vitro. *Investigative radiology* 39, 149-154 (2004).
50 Peer, A. *et al.* Contrast media augmented apoptosis of cultured renal mesangial, tubular, epithelial, endothelial, and hepatic cells. *Investigative radiology* 38, 177-182, doi:10.1097/01.rli.0000054529.61167.84 (2003).
51 SL, N. T. Reduced Graphene Oxide: Characterization sheet. (Nanoinnova Technologies SL, C/Faraday 7, 28049 Madrid).
52 Zhang, Y. *et al.* Cytotoxicity Effects of Graphene and Single-Wall Carbon Nanotubes in Neural Phaeochromocytoma-Derived PC12 Cells. *ACS Nano* 4, 3181-3186, doi:10.1021/nn1007176 (2010).
53 MD, M. M. in *The Trauma Professional's Blog* The Trauma Professional's Blog provides information on injury-related topics to trauma professionals. It is written by Michael McGonigal MD, the Director of Trauma Services at Regions Hospital in St. Paul, MN. Regions is a Level I Adult Trauma Center, and has partnered with Gillette Children's Specialty Hospital to become the first Level I Pediatric Trauma Center in the Upper Midwest. (Tumblr, 2012).
54 S, K. *et al.* Physicochemical characterization of a novel graphene-based magnetic resonance imaging contrast agent. *International Journal of Nanomedicine* 2013:8, 2821-2833, doi:http://dx.doi.org/10.2147/IJN.S47062 (2013).